



Kinetic and thermodynamic study on adsorption characteristics of ash derived from distilled waste of aromatic crop *Mentha piperita*: a low-cost, efficient adsorbent for crystal violet removal

Abhay Prakash Rawat, D.P. Singh*

Department of Environmental Sciences, Babasaheb Bhimrao Ambedkar University (A Central University), Lucknow, Uttar Pradesh, 226025, India, Tel. +91 9935078475; email: abhayprakashrawat@gmail.com (A.P. Rawat), Tel. +91 9415575735; email: dpsinghbbau@gmail.com (D.P. Singh)

Received 20 January 2017; Accepted 24 June 2017

ABSTRACT

The sorption potential of ash derived from extracted *Mentha piperita* plant was evaluated for removal of basic dye (crystal violet [CV]) from aqueous solution. Liquid batch methods were used to study the effect of various physico-chemical factors such as pH, initial dye concentration, contact time, temperature and adsorbent dose on the sorption efficiency of *Mentha Piperita* plant ash (MPA). Zeta potential of the MPA particles was calculated as -37.7 mV, indicating negatively charged sorption surface of MPA particles. Results on Freundlich and Langmuir equilibrium sorption isotherms showed that data fitted well to the Langmuir isotherm and the monolayer adsorption capacity (q_{\max}) was found to be 15.95 mg g⁻¹ at room temperature. Pseudo-first-order, pseudo-second-order kinetics and intra-particle diffusion were analyzed at different concentration of CV. The kinetic data fitted well with the pseudo-second-order kinetics as the value of calculated q_e in this model was found to be very close to experimental value of q_e . Activation energy (E_a) calculated for the surface binding of CV (14.90 kJ mol⁻¹) indicated that the dye binding by MPA was an energetically favourable physico-chemical sorption process. Results on the thermodynamic factors (ΔH° , ΔS° and ΔG°) showed the feasible, spontaneous and endothermic nature of adsorption. Further, use of desorbing agents like 0.1 N solution of HCl, H₂SO₄, CH₃COOH, NaOH and H₂O exhibited better recovery of CV from the MPA in the presence of HCl and H₂SO₄ than CH₃COOH, NaOH and H₂O.

Keywords: *Mentha piperita* plant ash; Waste water treatment; Crystal violet; Kinetics; Adsorption isotherms; Thermodynamics

1. Introduction

Among various industries, the textile industry stands first in the application of colouring dyes and is estimated that approximately 15% of the total dye stuff is lost in the industrial effluents during manufacturing operations [1,2]. Most of the dyes used in the textile industry are more stable against photobleaching and offer resistance against aerobic microbial degradation because of their complex nature and large size of molecules [3,4]. The crystal violet (CV), a triarylmethane dye, is a basic cationic dye mostly used in the textile industry,

manufacturing of paints and printing inks [5,6]. The CV has been considered as a persistent recalcitrant molecule in the environment as it is poorly metabolized by the microbes [6]. In addition to it, the CV is found to be relatively more carcinogenic, genotoxic, mutagenic and teratogenic as compared with anionic dyes due to its aromatic ring with delocalized electrons [7]. If the CV dye is absorbed in higher amounts through the skin, it can cause skin irritation, digestive tract irritation, respiratory and kidney failures [5,6,8,9].

The removal of CV dye from the waste water, before discharging them into the receiving water body, is the major concern of environmentalists [7]. Many of the conventional techniques such as coagulation, precipitation, filtration, solvent extraction, reverse osmosis, photocatalytic degradation

* Corresponding author.

including biodegradation have been tested for the treatment of dye-loaded industrial effluents [6,10]. Though, adsorption technique is a promising one for the removal of the dyes from the waste water, major concerns of this technology are the cost-effectiveness, adsorption efficiency, generation of by-products and environmental sustainability [6,11,12]. The removal of basic cationic dyes from aqueous solution has been tried by using commercially available activated charcoal [13,14], which is still considered a high priced product. This has led many researchers to look for some alternatively cheap, eco-friendly and efficient adsorbents [15,16]. In this regard, agricultural solid wastes are considered as easily available, inexpensive and eco-friendly adsorbents for removal of dyes from the aqueous solution [17]. Large number of researchers have tried use of agrowaste materials such as cotton carbon, coconut coir, saw dust, rice husk, bagasse and maize cob carbon, etc. [17–23] for the removal of dyes and heavy metals from waste water.

India is a major producer of mentha waste in the world, followed by China and Brazil. The oil extracted mentha plant residue is dried and used as a cheap source of fuel for heating of the oil distilling units. The resulting plant ash is left behind as by-product with no subsequent application. *Mentha piperita* plant ash (MPA) is an unattended waste by-product of Mentha distillation industry and it is easily available in the vicinity of the industrial plant. Thus, MPA with no additional cost and pre-treatment can be applied for removal of cationic dyes as it has negatively charged surface. The physico-chemical nature of adsorption and recovery of the dyes by using desorbing agents are the additional reasons for the selection of this material (MPA). Therefore, the main objective of present study was to evaluate the sorption potential of MPA as a low-price, efficient adsorbent for the removal of CV from aqueous solutions. Effect of different process optimization parameters such as pH, adsorbent dose and initial concentration of dye, contact time and temperature was studied to understand the nature of dye adsorption.

2. Materials and methods

2.1. Chemicals and solutions

The dye, CV, used in this study was purchased from S.D. Fine Chem Ltd. (Mumbai, India) (CI = 42535, molecular formula = $C_{25}H_{30}N_3Cl$, molecular weight = 408 g mol⁻¹, λ_{max} = 590 nm). Monobasic dihydrogen phosphate (KH_2PO_4 , 99.5%), dibasic monohydrogen phosphate (K_2HPO_4 , 99.0%), sodium borate ($Na_2B_4O_7 \cdot 10H_2O$), NaOH, citric acid and dibasic sodium phosphate ($Na_2HPO_4 \cdot 7H_2O$) were obtained from Himedia Labs Ltd., Chennai, India. The stock solution (1,000 mg L⁻¹) of CV dye was prepared using deionized water. Different concentrations of dye solution were prepared by appropriate dilution of the stock solution in 20 mM phosphate buffer (pH = 7.0) and further experiments were carried out under different physico-chemical conditions.

2.2. Collection and preparation of adsorbent

MPA, a by-product of the mentha oil production, was collected from local mentha oil distillation unit, Uttar Pradesh, India. Prior to use, MPA was kept in hot air oven at a temperature of 80°C for 6–8 h to remove the moisture

from material. The material was homogenized in the form of fine powder. The powder was sieved so that all the particles were of almost of similar size. Finally the MPA sample was filled in air tight bottles so that it can be used for future study without any pre-treatment.

2.3. Characterization of adsorbent

2.3.1. Zeta potential

Zeta potential analyzer (Malvern Instruments Ltd., (United Kingdom) Serial Number: MAL1010294) was used to determine the surface potential of MPA particles. The MPA sample was prepared by dissolving 1.0 mg of MPA in 10 mL distilled water and was sonicated before analysis. The zeta potential spectrum was recorded in the range of –200 to 200 mV.

2.3.2. SEM analysis

Scanning electron microscopy (SEM) (Model: JSM- 6490 LV JEOL, Japan) was used to characterize the surface morphology and some of the fundamental physical properties of MPA adsorbent. Images were taken at an accelerating voltage of 30 kV and resolution of 4,300×.

2.3.3. BET specific surface area

The Brunauer-Emmett-Teller (BET) specific surface area and other textural characteristics of MPA were determined using BET (BEL Master™ Ver. 2.3.1, BEL Japan, INC.). N₂ adsorption–desorption isotherm and Barrett-Joyner-Halenda (BJH) plot was measured on MPA at 77 K to find the shape of adsorption/desorption isotherm and porosity of the material, respectively.

2.3.4. IR spectroscopy

Fourier transform infrared spectroscopy (FTIR) (Thermo Scientific, USA; Model: Nicolet™ 6700) analysis of MPA particles, before and after adsorption of CV dye, was carried out to determine the nature of dye binding. The MPA particles (after and before dye binding) were dried in an oven at 80°C for 2–4 h and were mixed with 100 mg of spectroscopy grade potassium bromide (KBr). The pellet of mixture was made by using hydraulic press (capacity 15 t). The FTIR spectra were recorded in the range of 4,000 to 500 cm⁻¹. The spectra were corrected for KBr absorbance.

2.4. Sorption studies

Liquid batch experiments were conducted to investigate the sorption efficiency of MPA as a low-cost adsorbent for the removal of CV from aqueous solution. All the sorption experiments were conducted in 250 mL conical flasks containing 0.1 g/100 mL of MPA and dye solution (pH = 7.0) with desired concentration were kept in thermostat orbital shaker (Model UTS: 1.21) at 180 rpm. The effect of varying physico-chemical condition such as adsorbent dose (0.5–5 g L⁻¹), initial pH conditions (pH 4–10), initial dye concentration (0–30 mg L⁻¹) and temperature (20°C–50°C) on the dye sorption potential of MPA was studied using liquid batch methods. To study the effect of contact time and

equilibrium time for sorption of CV, an amount of 0.1 g of MPA was added in 100 mL of 25 mg L⁻¹ dye solution (pH=7.0) at room temperature (32°C). Due to excess alkalinity caused by the adsorbent (MPA) in aqueous solution, the pH range of dye solution (25 mg L⁻¹) was adjusted to pH 4.0, 5.0, 7.0, 9.0 and 10.0 by using appropriate citrate-phosphate, phosphate and borate buffer (20 mM, each) to study the effect of pH on sorption of CV dye. An amount of 0.1 g of MPA was added to the dye solution to start the adsorption process at room temperature (32°C). To study the effect of different concentrations of CV dye on the adsorption, 100 mL of dye solutions containing different initial concentrations of CV (5, 10, 15, 20, 25 and 30 mg L⁻¹) at neutral pH was prepared. The same experimental procedure was followed for recording the adsorption of dye. The selection of initial concentrations of dye (0–30 mg L⁻¹) was based on the use of initial dose of adsorbent (0.1 g/100 mL) and average time duration (0–60 min) required for complete removal of CV dye in the selected range of concentrations. To study the effect of adsorbent dose on sorption of CV, 100 mL solution containing 25 mg L⁻¹ dye at neutral pH was supplemented with varying adsorbent doses (0.05, 0.1, 0.15, 0.2, 0.3 and 0.5 g/100 mL). In order to study the effect of temperature on sorption of CV, the 100 mL experimental solution containing 25 mg L⁻¹ dye at neutral pH was placed under different temperature (20°C–50°C) for measurement of CV binding on MPA.

Small aliquots of sample (3.0 mL) were withdrawn at regular time interval and the samples were centrifuged (Remi Instruments Ltd. (Mumbai, India): AXCI-7182) at 5,000 rpm for 10 min to separate the dye-loaded adsorbent from the suspension. The final dye concentration in the supernatant was evaluated by measuring the concentration of dye at 590 nm, using a double beam UV–visible spectrophotometer (Shimadzu UV–1601). The amount of dye adsorbed at equilibrium, q_e (mg g⁻¹) and percentage removal were calculated by following equations:

$$q_e = \frac{(C_i - C_e)V}{m} \quad (1)$$

$$\text{Percent removal (\%)} = \frac{C_i - C_e}{C_i} \times 100 \quad (2)$$

where C_i (mg L⁻¹) and C_e (mg L⁻¹) are the initial and final dye concentration in solution, respectively, V is the volume of the working solution (L) and m is the mass of the adsorbent (g).

2.5. Adsorption isotherms

Langmuir and Freundlich equilibrium adsorption isotherms were used to describe the equilibrium experimental data for the sorption of CV onto MPA. Langmuir isotherm model [24] was applicable for the calculation of the maximum capacity of adsorption (q_{\max}) conforming to whole monolayer coverage on the surface of adsorbent. A plot of $1/q_e$ vs. $1/C_e$ was used to obtain Langmuir equilibrium isotherm. Value of q_{\max} (mg g⁻¹) and b was calculated from the slope and intercept of the plot. The Langmuir isotherm equation is given in linear form as:

$$\frac{C_e}{q_e} = \frac{1}{q_{\max} b} + \frac{C_e}{q_{\max}} \quad (3)$$

where C_e (mg L⁻¹) is the final dye concentration, q_e (mg g⁻¹) is the amount of dye uptake at equilibrium, q_{\max} (mg g⁻¹) is the Langmuir constant related to the maximum adsorption capacity and b (L mg⁻¹) is the adsorption energy. Equilibrium factor or separation factor (R_L) was used to express important characteristics of Langmuir equilibrium isotherm [25], which is given as below:

$$R_L = \frac{1}{1 + bC_i} \quad (4)$$

The Freundlich isotherm [26] was applicable in heterogeneous surface adsorption and can be written in linear form as:

$$\log q_e = \log K_f + 1/n \log C_e \quad (5)$$

where K_f (mg g⁻¹) is the adsorption capacity and n is the intensity of adsorption. Thus, a plot of $\log q_e$ vs. $\log C_e$ is a straight line and values of K_f and n are calculated from the intercept and slope of the linear plot.

2.6. Sorption kinetics

Pseudo-first-order and pseudo-second-order kinetic models were applied to know the extent of adsorption as a function of time. The amount of dye uptake at time t , q_t (mg g⁻¹), was calculated by the following equation:

$$q_t = \frac{(C_0 - C_t)V}{m} \quad (6)$$

where C_0 (mg L⁻¹) is the initial concentration of dye and C_t (mg L⁻¹) is the concentration of dye at time (t).

Pseudo-first-order kinetic model states that the rate of adsorption is proportional to the number of vacant sites [27], which can be described by the following equations:

$$d_t/d_i = K_1 (q_e - q_t) \quad (7)$$

A linear form of pseudo-first-order model was described in the form [28]:

$$\log(q_e - q_t) = \log q_e - K_1 t/2.303 \quad (8)$$

where q_e (mg g⁻¹) and q_t (mg g⁻¹) are adsorption capacity at equilibrium and after time (t), respectively, and K_1 (min⁻¹) is the first-order rate constant. The constants of pseudo-first-order kinetics can be calculated from the slope and intercept of the plot of $\log(q_e - q_t)$ vs. t . The value of intercept in the plot is equal to the $\log q_e$.

Pseudo-second-order kinetics can be written in a linear form as [15,19]:

$$\frac{t}{q_t} = \frac{1}{K_2 q_e^2} + \frac{t}{q_e} \quad (9)$$

where second-order rate constant K_2 ($\text{g mg}^{-1} \text{min}^{-1}$) and q_e were calculated from the intercept and slope of the plot t/q vs. t .

Pseudo-second-order kinetic model was also used to calculate initial adsorption rate h ($\text{mg g}^{-1} \text{min}^{-1}$) for the sorption of CV onto MPA, which can be written as:

$$h_{0,2} = K_2 q_e^2 \quad (10)$$

Intra-particle diffusion model was also studied to investigate the rate controlling steps and sorption mechanisms affecting the sorption kinetics [4]. Intra-particle diffusion model can be expressed as [29,15]:

$$q_t = K_{id} t^{1/2} + C \quad (11)$$

where C is the intercept and rate constant K_{id} ($\text{mg g}^{-1} \text{min}^{-1/2}$) of intra-particle diffusion can be evaluated from slope of the linear plot of q_t vs. $t^{1/2}$ [15].

2.7. Activation energy

The activation energy (E_a) for the sorption of CV by MPA was calculated using Arrhenius equation [11]:

$$\ln k = \ln A - \frac{E_a}{RT} \quad (12)$$

where k is the velocity constant, A is Arrhenius constant, E_a (kJ mol^{-1}) is the activation energy, R ($8.314 \text{ J mol}^{-1} \text{K}^{-1}$) and T (K) stands for gas constant and temperature, respectively. The value of velocity constant (k) was determined by the equation:

$$k = \frac{C_0}{C_f} \quad (13)$$

where C_0 (mg L^{-1}) and C_f (mg L^{-1}) are the initial and final concentration of CV dye in solution at temperature (K), respectively. Activation energy (E_a) was calculated from the slope of linear plot of $\ln k$ vs. $1/T$.

2.8. Thermodynamic study

If the adsorption is temperature dependent process, it is useful to define the thermodynamic factors such as enthalpy change (ΔH°), free energy change (ΔG°) and standard entropy change (ΔS°) [30]. In this investigation, the Gibbs free energy change for sorption of CV onto MPA as studied in a temperature range (293–323 K) as given below:

$$\Delta G = -RT \ln Kc \quad (14)$$

ΔH° and ΔS° of sorption process were calculated from Van't Hoff equation, which can be written as:

$$\ln Kc = \frac{\Delta S^\circ}{R} - \frac{\Delta H^\circ}{RT} \quad (15)$$

where Kc is equilibrium constant for sorption, R is the gas constant, T is absolute temperature (K). The value of ΔH° and ΔS° were calculated from the slope and intercept of the linear plot of $\ln Kc$ vs. $1/T$. The Kc value was determined by the following relation:

$$Kc = \frac{q_e}{C_e} \quad (16)$$

where q_e (mg g^{-1}) and C_e (mg L^{-1}) are the amount of CV adsorbed onto MPA at equilibrium and equilibrium concentration of CV in solution, respectively.

2.9. Desorption of dye

A study on desorption process was carried out to see the recovery of adsorbent as well as re-use potential of adsorbate. If the dye desorption occurred by desorbing agents such as acids (H_2SO_4 , HCl and CH_3COOH) or alkali (NaOH), it indicated chemisorption [31].

In the present desorption study, 100 mL of 25 mg L^{-1} CV dye solution was mixed with sorbent MPA at pH 7.0 and the resulting working solution was placed under shaking (180 rpm) at room temperature (32°C) for 75 min. The final dye concentration was measured. The dye-loaded MPA was separated by centrifugation and it was dried for 4–6 h at 70°C . An amount of 0.1 g of dried sample of MPA was transferred to 100 mL of each desorbing solution, that is 0.1 N HCl , CH_3COOH , H_2SO_4 , NaOH and H_2O . The percentage of desorbed dye was calculated at regular time interval by the equation:

$$\text{Percent desorption (\%)} = \frac{\text{Desorbed mass}}{\text{Adsorbed mass}} \times 100 \quad (17)$$

3. Results and discussion

3.1. Characterization of MPA adsorbent

The surface charge of MPA is considered an important factor in determining the adsorption capacity of adsorbent. In order to see the role of surface charge of adsorbent in dye adsorption, the zeta potential of MPA was calculated as -37.7 mV. Zeta potential curve of MPA sample has been shown in Fig. 1(a). Zeta potential of the adsorbent particles indicated that the surface of the MPA particles is negatively charged. A highly electronegative surface of adsorbent could be due to unburnt biomolecules and the minerals present in the MPA. The adsorbent used in the present investigation is natural by-product of the industrial process. However, negatively charged surface of MPA can be more suitable adsorbent for adsorption of cationic dyes like CV [32].

The surface morphology of MPA has been shown in Fig. 1(b). The SEM micrograph of MPA shows regular and spherical shapes of particles. Moreover, shape of the diversified MPA particles varies from regular spherical shapes to completely irregular shape. It is possible to find very large particles as well as much smaller ones. The size of MPA particles is recorded in the range of micrometers.

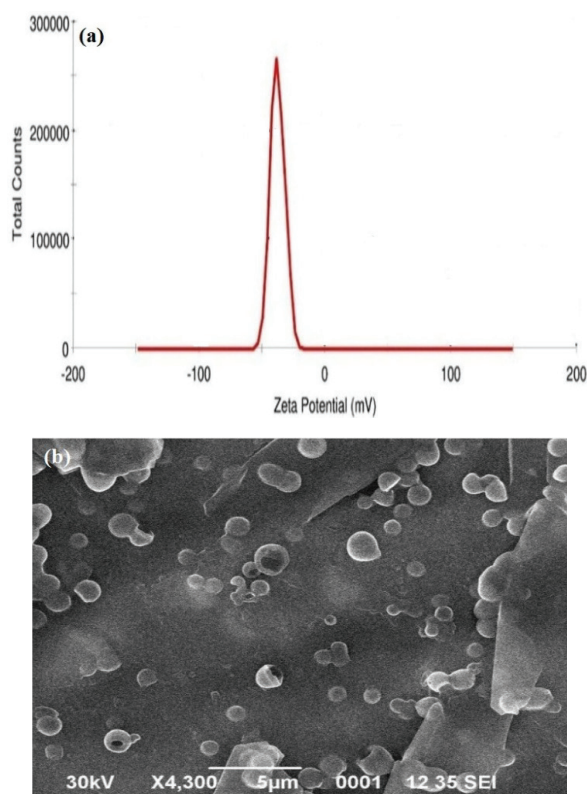


Fig. 1. (a) Zeta potential curve and (b) SEM image of MPA.

In the BET analysis of MPA particles, the shape of N_2 adsorption/desorption isotherm is considered to determine the specific surface area and porosity of the MPA particles. The shape of all the adsorption isotherms is usually categorized into five basic types (type I to V) [31]. Results on N_2 adsorption–desorption isotherm and BJH plot at 77 K (Figs. 2(a) and (b)), indicated type IV shape of adsorption isotherm and mesoporous nature of MPA, respectively. Type IV shape of adsorption isotherm shows comparatively strong interaction between surface of adsorbent and adsorbate. In the present study, the BET specific surface area, total pore volume and average pore diameter were found to be $7.149 \text{ m}^2 \text{ g}^{-1}$, $2.067 \text{ cm}^3 \text{ g}^{-1}$ and 11.582 nm , respectively. The pore diameter of MPA particle, as calculated by BJH method, was found to be 3.28 nm . It indicates that the MPA particle is mesoporous material. The International Union of Pure and Applied Chemistry classifies the mesopores ranging with diameter (d) between 2 and 50 nm, micropores ($d < 2 \text{ nm}$) and macropores ($d > 50 \text{ nm}$) [31]. The small BET specific surface area ($7.149 \text{ m}^2 \text{ g}^{-1}$) of MPA was perhaps due to filling of its pores largely with resins and minerals attributable to incomplete combustion, which interfere with the passage for nitrogen molecules.

The FTIR spectrum of adsorbent (MPA) between $4,000$ and 500 cm^{-1} is obtained to study the surface characteristics of adsorbent. A comparison of the IR spectra of MPA particles taken before and after adsorption of cationic CV dye shows the involvement of various electronegative functional groups present on the surface of MPA particles. The IR spectrum of CV dye–treated MPA sample shows stretching and bending vibrations of various functional groups, denoting their

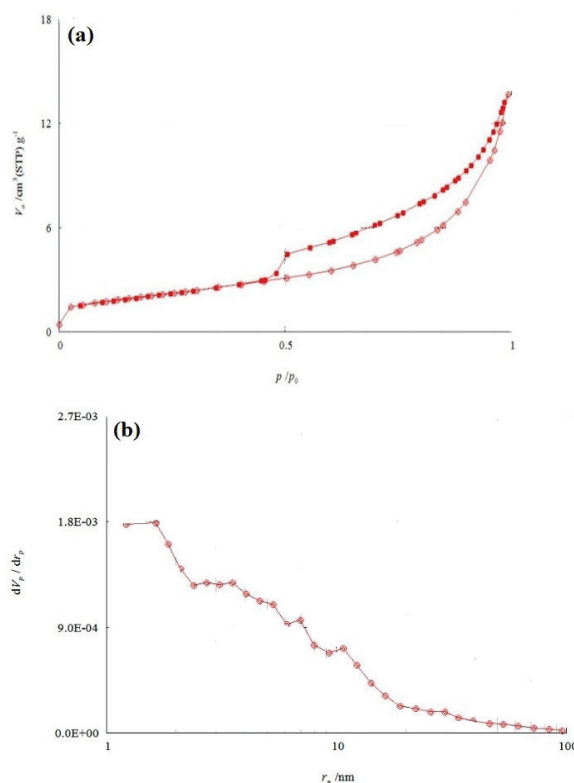


Fig. 2. (a) N_2 adsorption/desorption isotherm and (b) BJH plot measured on MPA at 77 K.

involvement in the adsorption process as given in Table 1 and Fig. 3. The changes in IR absorption peaks appearing at $3,694.3$ and $3,424.8 \text{ cm}^{-1}$ wavenumbers, assigned to O–H and amine groups, respectively, suggests the important role played by these functional groups in dye binding on the MPA surface. The results on IR absorption spectrum of MPA due to CV binding showed increased absorption area curve as well as shift in the IR peaks at wavenumbers $1,795.6$; $1,426.5$ and $1,040 \text{ cm}^{-1}$. These results indicate the role of acid chloride with C=O stretching [33] of amines, carboxylic and carbonyl groups, which play crucial role in CV binding by MPA particle. The band at $1,426.5$ and $1,040.9 \text{ cm}^{-1}$ are characteristic of C–O stretching and vibrations of lignin and carbohydrates as reported earlier [34] in wood samples. It has been suggested that the shift in the absorption peak at $1,040.9 \text{ cm}^{-1}$ to lower wavenumber $1,035.8 \text{ cm}^{-1}$ pertains to C–O stretching in carbohydrates [35]. The band at 898 cm^{-1} , assigned to the amorphous region in the cellulose, also changes after dye binding [36]. The overall results on IR spectra of MPA exhibit that hydroxyl, amine, ester, carbonyl groups including acid chloride are the functional moieties not only contributing to negative charge on surface of MPA but are also actively involved in the binding of cationic CV dye.

3.2. Effect of physico-chemical factors on adsorption

3.2.1. Effect of contact time

Dye removal by MPA particles was studied as a function of time with using fixed concentration of CV dye (25 mg L^{-1}) and dose of adsorbent ($0.1 \text{ g}/100 \text{ mL}$) (Fig. 4(a)). The dye

Table 1
FTIR wavenumber cm^{-1} of MPA adsorbent before and after adsorption of CV

Observed frequency in cm^{-1} of MPA adsorbent			
Frequency range (cm^{-1})	Before adsorption of CV dye	After adsorption of CV dye	Band assignment
3,800–3,550	3,694.3	0	O–H stretching of alcohol [37]
3,550–3,250	3,424.8	0	N–H stretching of amine [38]
3,200–2,500	2,514.0	0	O–H stretching of carboxylic acid [33]
1,815–1,770	1,795.6	0	C=O stretching of acid chloride [33]
1,435–1,405	1,426.5	1,434.2	C–O stretching of carbonyl compound [34]
1,300–1,000	1,040.9	1,035.8	C–O stretching of ester [37]
920–830	874.7	874.3	C–O out of plane bending of carbonate [39]
770–620	712.8	713.0	C–O in plane bending of carbonate [39]
	687.8	692.4	

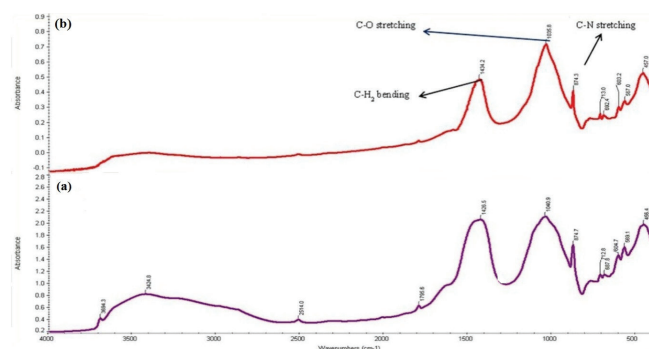


Fig. 3. FTIR (Mid) stack image of MPA (a) before and (b) after adsorption of crystal violet dye.

removal by MPA from ambient aqueous medium initially occurred at a faster rate, corresponding to 71.6% removal within 15 min. A rapid rate of initial dye removal by adsorbent could be due to maximum availability of vacant binding sites on the surface of adsorbent, ensuring high efficiency of dye removal as suggested by earlier workers [40]. The subsequent stage of slower rate of dye removal after about 15 min could be attributed to less availability of binding ligands on the surface of MPA. Earlier, workers have also demonstrated an initial fast phase, followed by slow phase due to saturation of available adsorption sites [41,42].

3.2.2. Effect of adsorbent dose

Adsorbent dosage is a critical factor in determination of extent of dye removal, depending upon adsorptive capacity of an adsorbent and operating conditions. The percentage removal of CV dye by MPA was studied as a function of varying adsorbent doses (0.05–0.5 g/100 mL) at fixed concentration of CV dye (25 mg L^{-1}) for 75 min. The results (Fig. 4(b)) showed a rapid phase of dose dependent increase in the dye removal up to 0.3 g/100 mL dose of MPA and that was followed a sluggish phase of dye removal between 0.3 and 0.5 g/100 mL of doses of adsorbent. The results clearly showed about 90% removal of dye at adsorbent dose of 0.3 g/100 mL. The biphasic pattern of dose dependent dye removal could be interpreted in terms of initial dose dependent rapid dye

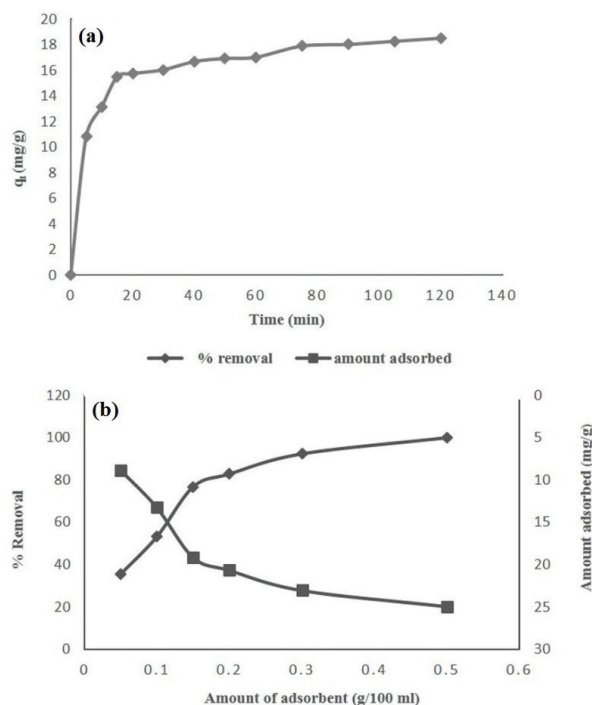


Fig. 4. (a) Effect of contact time on dye uptake (mg g^{-1}) by MPA. Conditions: $\text{pH} = 7$, $C_0 = 25 \text{ mg L}^{-1}$, $m = 0.1 \text{ g/100 mL}$, $T = 32^\circ\text{C}$. (b) Effect of adsorbent dose on amount adsorbed and percentage removal of CV. Conditions: $\text{pH} = 7$, $C_0 = 25 \text{ mg L}^{-1}$, $t = 90 \text{ min}$, $T = 32^\circ\text{C}$.

removal due to enhanced availability of dye binding ligands and larger surface area, while sluggish phase of dye removal might be the overlapping and shadowing effect of excess MPA particles on binding ligands and thereby, resulting into reduced accessibility of the dye molecules to the active site [8,9,43].

3.2.3. Effect of pH

Initial pH condition of the dye solution can influence the chemistry of dye as well as over all surface charge potential of the adsorbent [7]. Since variation in pH condition of the

solution leads to variation in the degree of ionization of the chemical moieties on the surface of adsorbent as well as ionization potential of adsorbate molecule [44]. In the present study, effect of different pH conditions (pH 4 to 10) on the dye binding property of MPA was assessed at fixed initial concentration of the CV dye (25 mg L^{-1}) and adsorbent dose ($0.1 \text{ g}/100 \text{ mL}$). The results (Fig. 5(a)) showed relatively lesser adsorption of dye at acidic pH (4.0), perhaps on account of reduced electronegative surface of MPA particles at acidic pH, which was not favourable for cationic dye. Besides, protonation of CV dye molecules at acidic pH also hinders the active binding between the adsorbent and adsorbate and thereby, reducing the adsorption capacity [45]. Further, the results on the pH dependent dye removal showed that a pH dependent gradual increase in the removal of CV dye between pH 4.0 to pH 10.0 is perhaps due to increased negatively charged functional groups on the surface of adsorbents. Earlier it has been reported that a greater electrostatic interaction between the cationic dye and electronegative surface of adsorbent facilitates faster rise in the dye adsorption [46,5].

3.2.4. Effect of initial dye concentration

The dye removal by MPA particles is highly dependent on the initial concentration of CV dye in aqueous solution. The effect of initial dye concentration on the sorption efficiency of MPA particles depend on the availability of dye

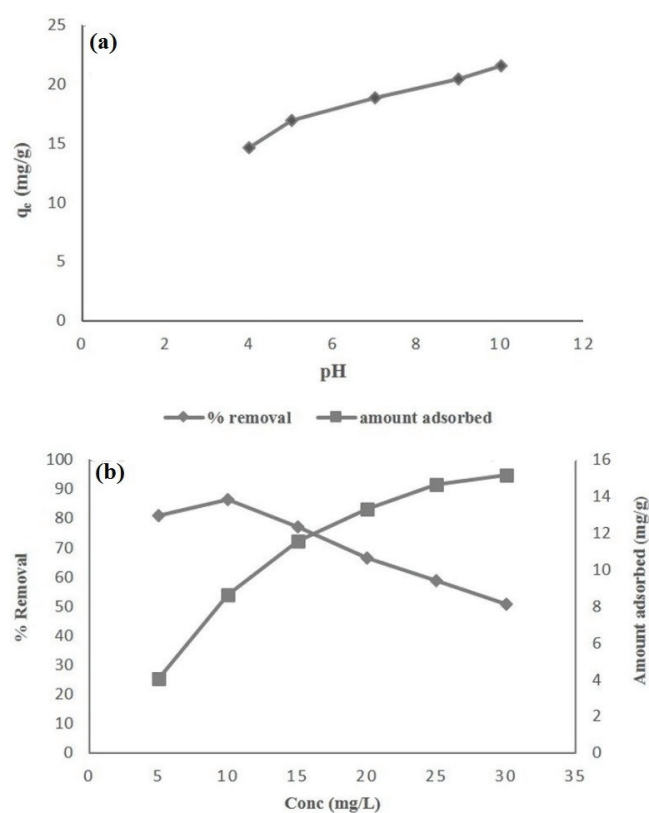


Fig. 5. (a) Effect of pH on dye uptake (mg g^{-1}) by MPA. Conditions: $C_0 = 25 \text{ mg L}^{-1}$, $T = 32^\circ\text{C}$, $t = 90 \text{ min}$, $m = 0.1 \text{ g}/100 \text{ mL}$. (b) Effect of different dye concentration on the sorption behaviour of MPA. Conditions: $\text{pH} = 7$, $m = 0.1 \text{ g}/100 \text{ mL}$, $T = 32^\circ\text{C}$, $t = 90 \text{ min}$.

molecules and active binding sites present on the surface of MPA particles [47]. The effect of different concentration of CV dye ($0\text{--}30 \text{ mg L}^{-1}$) on the sorption efficiency of MPA was studied, using fixed dose of adsorbent ($0.1 \text{ g}/100 \text{ mL}$) at room temperature and neutral pH (7.0). The present results (Fig. 5(b)) showed an initial concentration dependent rapid increase in the rate of CV removal up to 15 min. The saturating rate of dye adsorption at equilibrium (q_e) was found to increase from 4.05 to 15.19 mg g^{-1} with increase in the dye concentration from 5 to 30 mg L^{-1} . With increasing concentration of adsorbate (CV dye), the adsorption capacity of MPA increased, but percentage removal efficiency decreased, perhaps due to relatively higher driving force for mass transfer [47]. At higher concentrations of dye, the dye removal declined, perhaps due to reduced availability of adsorption sites on the surface of MPA as well as mass transfer resistances between the aqueous and solid phase [15]. The similar result has been reported in removal of methylene blue (MB) by pine leaves by other investigators [46].

3.3. Adsorption isotherms

The linear plot of $1/q_e$ vs. $1/C_e$ (Fig. 6(a)) showed better applicability of Langmuir isotherm model for the sorption of CV dye by MPA. The Langmuir constants q_{max} and b (Table 3) were calculated from the slope and intercept of the plot. The maximum monolayer sorption capacity (q_{max}) calculated from Langmuir isotherm model was found to be 15.95 mg g^{-1} at room temperature. This calculated q_{max} value was very close to experimental q_e value.

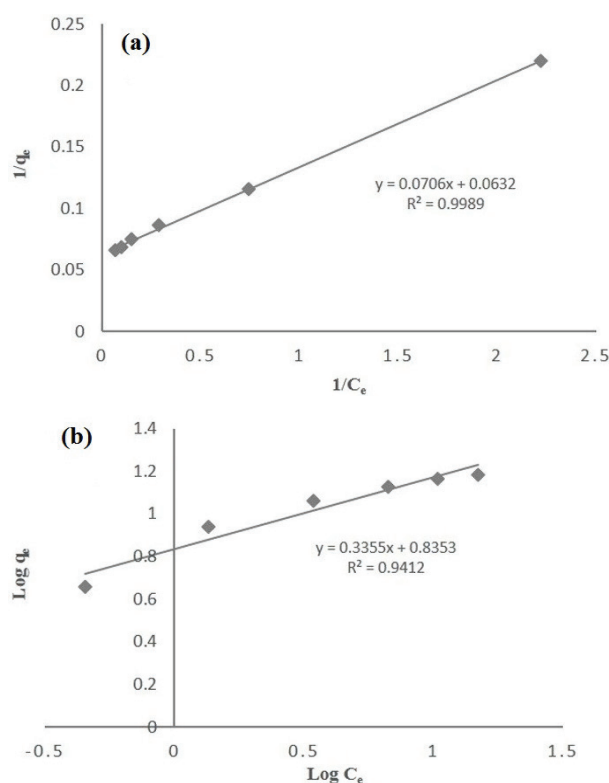


Fig. 6. (a) Langmuir and (b) Freundlich adsorption isotherms for the sorption of CV by MPA.

The applicability of Langmuir isotherm can be expressed better by determining the separation factor (R_L). The R_L value indicated the shape of Langmuir isotherm to be either linear ($R_L = 1$), favourable ($0 < R_L < 1$), unfavourable ($R_L > 1$) or irreversible ($R_L = 0$) [48,15]. The values of R_L (Table 2) between 0.183 and 0.036 at room temperature for dye concentration (5–30 mg L⁻¹), indicating favourable adsorption process of CV onto MPA.

The Freundlich constants K_f and n (Table 3) were calculated from the intercept and slope of the plot of $\log q_e$ vs. $\log C_e$ (Fig. 6(b)). The value of constant n between 1 and 10 indicated beneficial adsorption process [6]. The value of n in the present investigation was found to be 2.99 at room temperature, indicating beneficial adsorption process for the sorption of CV onto MPA.

In order to see the accuracy of the models, the correlation coefficient values (R^2) were calculated for both the isotherms as listed in Table 3. Analysis of the correlation coefficient ($R^2 > 0.999$) and equilibrium sorption data indicated that Langmuir isotherm model fitted quite well with experimental data, whereas, low correlation coefficient ($R^2 < 0.942$) showed poor agreement of Freundlich isotherm model with the experimental data. The q_{max} value of different sorbent materials, as given in Table 4, was used to compare our results. A comparison of sorption capacity of different adsorbents suggested that MPA was a better adsorbent than many other reported adsorbents.

3.4. Adsorption kinetics

The Lagergren’s first-order rate constants k_1 and q_e were calculated from the intercept and slope of the plot of $\log(q_e - q_t)$ vs. t (Fig. 7(a)) and listed in Table 5 along with their correlation coefficients (R^2). The value of pseudo-first-order rate constant (k_1) was found in a range of 0.058 to 0.023 for the sorption of CV onto MPA. Further, it was observed that calculated q_e values do not agree with experimental q_e values and the correlation coefficients ($R^2 > 0.88$) at different initial

Table 2
Equilibrium parameter or separation factor for MPA in the sorption of CV

Initial concentration (mg L ⁻¹)	Separation factor (R_L)
5	0.183
10	0.101
15	0.071
20	0.053
25	0.043
30	0.036

Table 3
Equilibrium adsorption constants for the sorption of CV by MPA

Langmuir constants			Freundlich constants		
q_{max} (mg g ⁻¹)	b (L mg ⁻¹)	R^2	n	K_f (mg g ⁻¹)	R^2
15.95	0.895	0.999	2.99	0.147	0.942

dye concentration also suggested that the pseudo-first-order kinetic model did not fit well to experimental data.

In pseudo-second-order kinetics, the rate constants k_2 and q_e were determined from the intercept and slope of the plot between t/q_t and t (Fig. 7(b)) and presented in Table 5 with their R^2 values. The rate constant (k_2) was found

Table 4
Comparison of adsorption capacity of MPA with other reported agro and plant wastes for CV

Adsorbents	q_m (mg g ⁻¹)	References
Banana peel	7.9	[49]
Rice husk (H ₂ SO ₄ activated)	64.87	[50]
Coniferous pinus bark powder	32.78	[8]
Bagasse fly ash	26.23	[31]
Jute fibre carbon	27.99	[51]
Ginger Waste	19.8	[52]
Rice bran	42.25	[53]
NaOH-modified rice husk	44.87	[6]
Sugaun saw dust	4.25	[54]
Sugarcane dust	3.8	[55]
Coir pith	2.56	[56]
MPA	15.95	This study

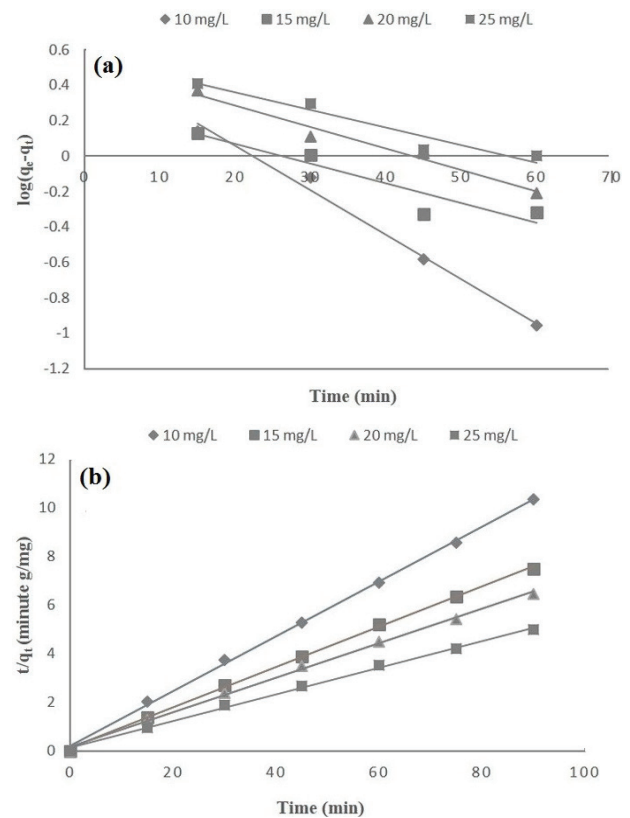


Fig. 7. (a) Pseudo-first-order and (b) pseudo-second-order kinetic model for the sorption of CV.

Table 5
Kinetic parameters obtained at different initial concentration of crystal violet dye

Dye conc. (mg L ⁻¹)	Exp. q_e (mg g ⁻¹)	First-order kinetics			Second-order kinetics			Intra-particle diffusion model			
		k_1 (min ⁻¹)	Cal. q_e (mg g ⁻¹)	R^2	k_2 (mg g ⁻¹ min ⁻¹)	Cal. q_e (mg g ⁻¹)	R^2	h (mg g ⁻¹ min ⁻¹)	K_{id} (mg g ⁻¹ min ^{-1/2})	C	R^2
10	8.69	0.058	1.8	0.989	0.062	8.88	0.998	4.89	0.25	6.65	0.881
15	12.02	0.026	3.47	0.878	0.052	12.05	0.998	7.56	0.24	9.79	0.964
20	13.94	0.029	1.9	0.973	0.03	14.11	0.997	5.98	0.41	10.19	0.973
25	18.02	0.023	1.81	0.931	0.024	18.22	0.997	7.97	0.48	13.58	0.97

in the range of 0.062–0.024 for the sorption of CV by MPA. The comparatively high values of correlation coefficients ($R^2 > 0.99$) at different initial dye concentration were much closer to unity, and calculated q_e values were also very closer to experimental q_e values. These results suggested that kinetic experimental values showed close-fitting to the pseudo-second-order kinetic model at room temperature. Similar observations were reported in the sorption of MB dye [57].

The observations on initial adsorption rate (h) showed that value of h increased from 4.89 to 7.97 mg g⁻¹ min⁻¹ (Table 5) with increasing dye concentration from 10 to 25 mg L⁻¹ which might be due to increase in driving force for mass transfer at high initial dye concentration [15]. An increasing trend of h values with the increasing dye concentration might be due to higher rate of dye binding at lower concentration of dye. High h values (7.97 mg g⁻¹ min⁻¹) at rate saturating concentration of dye indicated that the adsorption of CV onto MPA might be carried out through surface interchange reactions until all the functional binding sites were occupied [58]. Similar observations were reported by other investigators [15,59].

In intra-particle diffusion model, a plot of q_t vs. $t^{1/2}$ showed linear regression and the line passes through the origin at each concentration of CV dye, indicated that the role of intra-particle diffusion could be the rate controlling step. The calculated values of intra-particle diffusion coefficient K_{id} and intercept C are presented in Table 5. A larger intercept (C) value in the linear plot indicated greater role of the surface sorption and lesser role of boundary layer diffusion [15]. At higher concentration of dye (25 mg L⁻¹), a higher value of C (13.58) was indicative of more surface sorption and reduced boundary layer diffusion effect. However, the linear plot at different concentration did not pass through the origin, clearly indicating that intra-particle diffusion was not the sole rate controlling factor as suggested earlier by other workers [60,15].

3.5. Activation energy

The activation energy (E_a) involved in the surface adsorption of dye was calculated from the slope of Arrhenius plot between $\ln k$ vs. $1/T$ (Fig. 8(a)). The activation energy of the surface binding process was calculated to be 14.90 kJ mol⁻¹ for dye binding by MPA, which confirmed the physico-chemical sorption process. The lower value of activation energies (>4 kJ mol⁻¹) has been reported to be

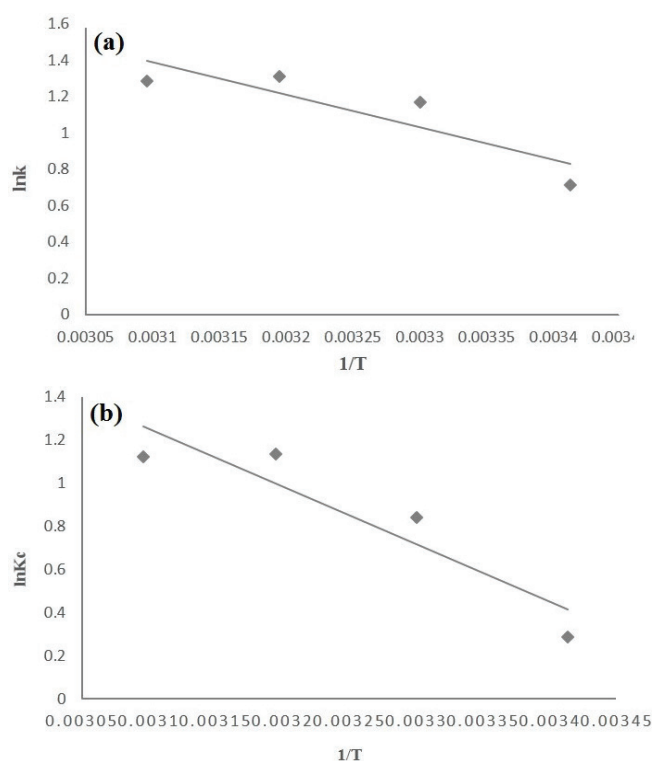


Fig. 8. (a) Arrhenius plot (b) Van't Hoff plot for the sorption of CV onto MPA.

responsible for physical adsorption, while higher value of E_a in the present study suggested for either activated chemisorption or mixture of both physical and activated chemisorption as suggested earlier [11].

3.6. Thermodynamic study

In the present experiment, the dye binding was recorded at different temperature from 293 to 323 K. The amount of adsorption increased from 14.29 to 18.91 mg g⁻¹ with rise in temperature, indicated endothermic adsorption process, where increased kinetic mobility of dye molecules to the active binding might have enhanced with increase in temperature. On the other hand, a decline in the adsorption capacity with the increasing temperature, an indicator of exothermic adsorption process, might be due to decrease in adsorptive forces between the dye molecules and active

binding sites as suggested earlier [61]. In the present investigation, temperature dependent increase in adsorption capacity of the adsorbent could be due to enhanced number of surface active centres available for adsorption [62]. Results in Table 6 showed negative values of ΔG° (from -0.703 to -3.014 kJ mol $^{-1}$) at all the chosen temperatures, which indicated that the adsorption of CV dye onto MPA particle was thermodynamically feasible and spontaneous. The Gibb's free energy change with negative value for adsorption supported that view that the adsorption of CV dye was a favourable adsorption process. An increase in the negative value of ΔG° with rising temperature specified that the adsorption process was more favourable at lower temperature [11]. A plot of $\ln K_c$ vs. $1/T$ (Fig. 8(b)) was used to calculate the enthalpy (ΔH°) and entropy (ΔS°) values. The results showed a positive value of ΔH° (22.25 kJ mol $^{-1}$), indicating that the adsorption process was endothermic and nature of interaction between the MPA particles and dye molecules was a physico-chemical process. The endothermic nature of CV sorption by surface moieties on MPA particles might be deriving the required energy from hydration shell of dye molecules [30]. The positive value of ΔS° (79.37 J mol $^{-1}$ K $^{-1}$) was supporting involvement of hydration energy with the cationic dye and the same was released during the sorption of dye molecules, contributing to an increase in the degree of freedom of the water molecules [30,63].

3.7. Desorption of dye

The mineral acids (0.1 N HCl and H₂SO₄) were found to be more effective for desorption of dye from dye-loaded MPA as compared with other desorbing agents (Table 7). A high percentage of desorption (53.71%) occurred with mineral acid (HCl). Addition of HCl reduced the pH of solution and hence, at low pH (>5.0), the surface of MPA become more protonated and the attachment between dye molecules and MPA become weakened [31]. The desorption of dye

Table 6
Thermodynamic parameters for the sorption of CV onto MPA

T (K)	ΔG° (kJ mol $^{-1}$)	ΔH° (kJ mol $^{-1}$)	ΔS° (J mol $^{-1}$ K $^{-1}$)
293	-0.703	22.25	79.37
303	-2.121		
313	-2.949		
323	-3.014		

Table 7
Percentage desorption (%) of dye in different desorbing agents

Desorption solution (0.1 N)	Desorbed mass of dye (mg g $^{-1}$)	% desorption
CH ₃ COOH	3.38	18.6
H ₂ SO ₄	6.37	35.06
HCl	9.76	53.71
H ₂ O	3.78	20.8
NaOH	2.16	11.89

by mineral acid (HCl) indicated that the dye was adsorbed onto MPA by physico-chemical sorption [31]. But addition of H₂SO₄, NaOH and H₂O showed lower percentage CV desorption which might be due to formation of some colourless complex compounds as suggested by earlier workers [31].

4. Advantages and disadvantages

MPA is a waste by-product of Mentha distillation industry and it is easily available in the vicinity of the industrial plant. Thus, MPA with no additional cost and pre-treatment can be applied for removal of cationic dyes as it has negatively charged surface. The physico-chemical nature of adsorption and recovery of the dyes by using desorbing agents are additional advantages of the process. It also has the potential of being used as mixed cake of several other adsorbents for efficient treatment of waste water. However, application of MPA in aqueous media tends to cause enhancement in the alkalinity of media and offers a challenge for its safe disposal. The shelf life of MPA is fairly very long as it has less ash content and is rich in minerals and thus, it is non-biodegradable.

5. Conclusion

MPA, is a locally available, low-cost material, which can be used as an adsorbent for the removal of CV and other similar cationic dyes from the waste water without any pre-treatment. The adsorption of CV is found to be depended on dose of MPA (adsorbent), pH condition and contact time. The maximum adsorption capacity (q_{max}) of MPA was 15.95 mg g $^{-1}$ after 75 min of contact time at neutral pH (7.0) and room temperature (303 K). The changes in the IR peaks after dye binding with MPA indicated an interaction between the CV dye and binding ligands present on the surface of MPA. The adsorption isotherms and kinetics applied on the dye removal by MPA revealed monolayer adsorption of dye, following pseudo-second-order kinetics. Thermodynamic parameters on CV dye binding by MPA clearly indicated spontaneous and endothermic nature of chemisorption process. Finally it was concluded that the MPA, without any pre-treatment, is a cheap, eco-friendly adsorbent material exhibiting great adsorption potential for the removal of the cationic dye, which can be proven to be better than any costly commercial adsorbents available in the market.

Acknowledgements

The authors would like to acknowledge the Head, Department of Environmental Science and Director, University Science Instrumentation Centre (USIC), Babasaheb Bhimrao Ambedkar University, Lucknow, India, for providing laboratory facility to perform the experiments. The authors were grateful to the UGC, New Delhi, for providing RGNF to Mr. Abhay P. Rawat.

References

- [1] M. Auta, B.H. Hameed, Preparation of waste tea activated carbon using potassium acetate as an activating agent for adsorption of Acid Blue 25 dye, Chem. Eng. J., 171 (2011) 502–509.

- [2] A. Khaled, A. El Nembr, A. El-Sikaily, O. Abdelwahab, Removal of Direct N Blue-106 from artificial textile dye effluent using activated carbon from orange peel: adsorption isotherm and kinetic studies, *J. Hazard. Mater.*, 165 (2009) 100–110.
- [3] A.R. Dincer, Y. Gunes, N. Karakaya, E. Gunes, Comparison of activated carbon and bottom ash for removal of reactive dye from aqueous solution, *Bioresour. Technol.*, 98 (2007) 834–839.
- [4] W.J. Weber, J.C. Morris, *Advances in Water Pollution Research: Removal of Biologically Resistant Pollutant from Waste Water by Adsorption*, International Conference on Water Pollution Symposium, Vol. 2, Pergamon, Oxford, 1962, pp. 231–266.
- [5] A. Mittal, J. Mittal, A. Malviya, D. Kaur, V.K. Gupta, Adsorption of hazardous crystal violet from wastewater by waste materials, *J. Colloid Interface Sci.*, 343 (2010) 463–473.
- [6] S. Chakraborty, S. Chowdhury, P.D. Saha, Adsorption of crystal violet from aqueous solution onto NaOH-modified rice husk, *Carbohydr. Polym.*, 86 (2011) 1533–1541.
- [7] H. Shayesteh, A.R. Kelishami, R. Norouzebeigi, Adsorption of malachite green and crystal violet cationic dyes from aqueous solution using pumice stone as a low-cost adsorbent: kinetic, equilibrium and thermodynamic studies, *Desal. Wat. Treat.*, 57 (2016) 12822–12831.
- [8] R. Ahmad, Studies on adsorption of crystal violet dye from aqueous solution onto coniferous pinus bark powder (CPBP), *J. Hazard. Mater.*, 171 (2009) 767–773.
- [9] A. Saeed, M. Sharif, M. Iqbal, Application potential of grapefruit peel as dye sorbent: kinetics, equilibrium and mechanism of crystal violet adsorption, *J. Hazard. Mater.*, 179 (2010) 564–572.
- [10] M. Rafatullah, O. Sulaiman, R. Hashim, A. Ahmad, Adsorption of methylene blue on low-cost adsorbents: a review, *J. Hazard. Mater.*, 177 (2010) 70–80.
- [11] S. Chowdhury, P. Saha, Sea shell powder as a new adsorbent to remove Basic Green 4 (Malachite Green) from aqueous solutions: equilibrium, kinetic and thermodynamic studies, *Chem. Eng. J.*, 164 (2010) 168–177.
- [12] P. Saha, S. Chowdhury, S. Gupta, I. Kumar, Insight into adsorption equilibrium, kinetics and thermodynamics of malachite green onto clayey soil of Indian origin, *Chem. Eng. J.*, 165 (2010) 874–882.
- [13] B.H. Hameed, A.T.M. Din, A.L. Ahmad, Adsorption of methylene blue onto bamboo-based activated carbon: kinetics and equilibrium studies, *J. Hazard. Mater.*, 141 (2007) 819–825.
- [14] D. Kavitha, C. Namasivayam, Experimental and kinetic studies on methylene blue adsorption by coir pith carbon, *Bioresour. Technol.*, 98 (2007) 14–21.
- [15] B.H. Hameed, D.K. Mahmoud, A.L. Ahmad, Equilibrium modeling and kinetic studies on the adsorption of basic dye by a low-cost adsorbent: coconut (*Cocosnucifera*) bunch waste, *J. Hazard. Mater.*, 158 (2008) 65–72.
- [16] Z. Aksu, Application of biosorption for the removal of organic pollutants: a review, *Process Biochem.*, 40 (2005) 997–1026.
- [17] K. Kadirvelu, M. Kavipriya, C. Karthika, M. Radhika, N. Vennilamani, S. Pattabhi, Utilization of various agricultural wastes for activated carbon preparation and application for the removal of dyes and metal ions from aqueous solutions, *Bioresour. Technol.*, 87 (2003) 129–132.
- [18] V.K. Garg, R. Gupta, A.B. Yadav, R. Kumar, Dye removal from aqueous solution by adsorption on treated sawdust, *Bioresour. Technol.*, 89 (2003) 121–124.
- [19] P.K. Malik, S.K. Saha, Oxidation of direct dyes with hydrogen peroxide using ferrous ion as catalyst, *Sep. Purif. Technol.*, 31 (2003) 241–250.
- [20] S.T. Ong, C.K. Lee, Z. Zainal, Removal of basic and reactive dyes using ethylenediamine modified rice hull, *Bioresour. Technol.*, 98 (2007) 2792–2799.
- [21] K.S. Bharathi, S.T. Ramesh, Equilibrium, thermodynamic and kinetic studies on adsorption of a basic dye by *Citrullus lanatus* rind, *Iran. J. Energy Environ.*, 3 (2012) 23–34.
- [22] S.Y. Wong, Y.P. Tan, A.H. Abdullah, S.T. Ong, The removal of basic and reactive dyes using quarterised sugar cane bagasse, *J. Phys. Sci.*, 20 (2009) 59–74.
- [23] C. Namasivayam, D. Kavitha, Removal of Congo red from water by adsorption on to activated carbon prepared from coir pith, an agricultural solid waste, *Dyes Pigm.*, 54 (2002) 47–58.
- [24] M.D. Meitei, M.N.V. Prasad, Adsorption of Cu (II), Mn (II) and Zn (II) by *Spirodela polyrhiza* (L.) Schleiden: equilibrium, kinetic and thermodynamic studies, *Ecol. Eng.*, 71 (2014) 308–317.
- [25] K.R. Hall, L.C. Eagleton, A. Acrivos, T. Vermeulen, Pore solid diffusion kinetics in fixed bed adsorption under constant pattern conditions, *Ind. Eng. Chem. Fundam.*, 5 (1966) 212–223.
- [26] M. Hema, S. Arivoli, Adsorption kinetics and thermodynamics of malachite green dye onto acid activated low cost carbon, *J. Appl. Sci. Environ. Manage.*, 12 (2008) 43–51.
- [27] Y. Liu, Y.I. Liu, Biosorption isotherms, kinetics and thermodynamics, *Sep. Purif. Technol.*, 61 (2007) 229–242.
- [28] S. Lagergren, Zurtheorie der sogenannten adsorption gelosterstoffe, *K. Sven. Vetensk.akad. Handl.*, 24 (1898) 1–39.
- [29] M.M. Abd El-Latif, A.A. Ibrahim, M.M.F. El-Kady, Adsorption equilibrium, kinetics and thermodynamics of methylene blue from aqueous solutions using biopolymer oak sawdust composite, *J. Am. Sci.*, 6 (2010) 267–283.
- [30] R. Ahmad, R. Kumar, Adsorption studies of hazardous malachite green onto treated ginger waste, *J. Environ. Manage.*, 91 (2010) 1032–1038.
- [31] I.D. Mall, V.C. Srivastava, N.K. Agarwal, Removal of Orange-G and Methyl Violet dyes by adsorption onto bagasse fly ash – kinetic study and equilibrium isotherm analysis, *Dyes Pigm.*, 69 (2006) 210–223.
- [32] M.S. Bootharaju, T. Pradeep, Facile and rapid synthesis of a dithiol-protected Ag₂₅ quantum cluster for selective adsorption of cationic dyes, *Langmuir*, 29 (2013) 8125–8132.
- [33] J. Mohan, *Organic Spectroscopy Principles and Applications*, 2nd ed., Narosa Publishing House, New Delhi, 2005.
- [34] M. Poletto, A.J. Zattera, R.M.C. Santana, Structural differences between wood species: evidence from chemical composition, FTIR spectroscopy and thermogravimetric analysis, *J. Appl. Polym. Sci.*, 126 (2012) 336–343.
- [35] S.G. Reznik, I. Katz, C.G. Dosoretz, Removal of dissolved organic matter by granular activated carbon adsorption as a pretreatment to reverse osmosis of membrane bioreactor effluents, *Water Resour.*, 42 (2008) 1595–1605.
- [36] M. Akerholm, B. Hinterstoisser, L. Salmen, Characterization of the crystalline structure of cellulose using static and dynamic FT-IR spectroscopy, *Carbohydr. Res.*, 339 (2004) 569–578.
- [37] J.R. Mohrig, C.N. Hammond, P.F. Schatz, *Techniques in Organic Chemistry*, 3rd ed., W.H. Freeman and Company, New York, 2006.
- [38] B.S.A. Farhan, Potential removal of crystal violet (CV), Acid Red (AR) and Methyl Orange (MO) from aqueous solution by magnetic nanoparticles, *Int. J. Nanomater. Chem.*, 3 (2015) 97–102.
- [39] E. Smidt, M. Schwanninger, Characterization of waste materials using FT-IR Spectroscopy – process monitoring and quality assessment, *Spectrosc. Lett.*, 38 (2005) 247–270.
- [40] T.K. Sen, M.V. Sarzali, Removal of cadmium metal ion (Cd²⁺) from its aqueous solution by aluminium oxide (Al₂O₃): a kinetic and equilibrium study, *Chem. Eng. J.*, 142 (2008) 256–262.
- [41] V.K. Verma, A.K. Mishra, Removal of dyes using low cost adsorbents, *Ind. J. Chem. Technol.*, 15 (2008) 140–145.
- [42] C.A. Basar, Y. Onal, T. Kilicer, D. Eren, Adsorptions of high concentration malachite green by two activated carbons having different porous structures, *J. Hazard. Mater.*, 127 (2005) 73–80.
- [43] V.K. Garg, R. Kumar, R. Gupta, Removal of malachite green dye from aqueous solution by adsorption using agro-industry waste: a case study of *Prosopis cineraria*, *Dyes Pigm.*, 62 (2004) 1–10.
- [44] B.K. Nandi, A. Goswami, M.K. Purkait, Removal of cationic dyes from aqueous solutions by kaolin: kinetic and equilibrium studies, *Appl. Clay Sci.*, 42 (2009) 583–590.
- [45] M.C. Ncibi, B. Mahjoub, M. Seffen, Kinetic and equilibrium studies of methylene blue biosorption by *Posidonia oceanica* (L.) fibres, *J. Hazard. Mater.*, 139 (2007) 280–285.
- [46] M.T. Yagub, T.K. Sen, H.M. Ang, Equilibrium, kinetics and thermodynamics of methylene blue adsorption by pine tree leaves, *Water Air Soil Pollut.*, 223 (2012) 5267–5282.
- [47] Y. Bulut, H. Aydın, A kinetics and thermodynamics study of methylene blue adsorption on wheat shells, *Desalination*, 194 (2006) 259–267.

- [48] V.K. Gupta, S.K. Srivastava, D. Mohan, Equilibrium uptake, sorption dynamics, process optimization, and column operations for the removal and recovery of malachite green from wastewater using activated carbon and activated slag, *Ind. Eng. Chem. Res.*, 36 (1997) 2207–2218.
- [49] G. Annadurai, R.S. Juang, D.J. Lee, Use of cellulose-based wastes for adsorption of dyes from aqueous solutions, *J. Hazard. Mater.*, 92 (2002) 263–274.
- [50] K. Mohanty, J.T. Naidu, B.C., Meikap, M.N. Biswas, Removal of crystal violet from waste water by activated carbons prepared from rice husk, *Ind. Eng. Chem. Res.*, 45 (2006) 5165–5171.
- [51] K. Porkodi, K.V. Kumar, Equilibrium kinetics and mechanism modeling and simulation of basic and acid dyes sorption onto jute fiber carbon: eosin yellow malachite green and crystal violet single component systems, *J. Hazard. Mater.*, 143 (2007) 311–327.
- [52] R. Kumar, R. Ahmad, Biosorption of hazardous crystal violet dye from aqueous solution onto treated ginger waste (TGW), *Desalination*, 265 (2011) 112–118.
- [53] X.S. Wang, X. Liu, L. Wen, Y. Zhou, Z. Li, Comparison of basic dye crystal violet removal from aqueous solution by low-cost biosorbents, *Sep. Sci. Technol.*, 43 (2008) 3712–3731.
- [54] S.D. Khattri, M.K. Singh, Use of Sagaun sawdust as an adsorbent for the removal of crystal violet dye from simulated wastewater, *Environ. Progr. Sustain. Energy*, 31 (2012) 435–442.
- [55] S.D. Khattri, M.K. Singh, Colour removal from synthetic dye wastewater using a biosolid sorbent, *Water Air Soil Pollut.*, 120 (2009) 283–294.
- [56] C. Namasivayam, M.D. Kumar, K. Selvi, R.A. Begum, T. Vanathi, R.T. Yamuna, Waste coir pith – a potential biomass for the treatment of dyeing wastewaters, *Biomass Bioenergy*, 6 (2001) 477–483.
- [57] E.S. Abechi, C.E. Gimba, A. Uzairu, J.A. Kagbu, Kinetics of adsorption of methylene blue onto activated carbon prepared from palm kernel shell, *Arch. Appl. Sci. Res.*, 3 (2011) 154–164.
- [58] H. Ma, J.B. Li, W.W. Liu, M. Miao, B.J. Cheng, S.W. Zhu, Novel synthesis of a versatile magnetic adsorbent derived from corn cob for dye removal, *Bioresour. Technol.*, 190 (2015) 13–20.
- [59] K.V. Kumar, Linear and non-linear regression analysis for the sorption kinetics of methylene blue onto activated carbon, *J. Hazard. Mater.*, 137 (2006) 1538–1544.
- [60] A.S. Alzaydien, Adsorption of methylene blue from aqueous solution onto a low cost natural Jordanian Tripoli, *Am. J. Environ. Sci.*, 5 (2009) 197–208.
- [61] M.A.M. Salleh, D.K. Mahmoud, W.A.W.A. Karim, A. Idris, Cationic and anionic dye adsorption by agricultural solid wastes: a comprehensive review, *Desalination*, 280 (2011) 1–13.
- [62] S.V. Mohan, N.C. Rao, J. Karthikeyan, Adsorptive removal of direct azo dye from aqueous phase onto coal based sorbents: a kinetic and mechanistic study, *J. Hazard. Mater.*, 90 (2002) 189–204.
- [63] J. Ghasemi, S. Asadpour, Thermodynamics' study of the adsorption process of methylene blue on activated carbon at different ionic strengths, *J. Chem. Thermodyn.*, 39 (2007) 967–971.